Adaptive Vehicle Traction Force Control for Intelligent Vehicle Highway Systems (IVHSs)

Hyeongcheol Lee and Masayoshi Tomizuka, *Fellow, IEEE*

***Abstract*—This paper is concerned with robust longitudinal control of vehicles in intelligent vehicle highway systems by adaptive vehicle traction force control. Two different traction force controllers, adaptive fuzzy logic control and adaptive sliding-mode control, are proposed and applied to the fastest stable acceleration/deceleration and robust vehicle platooning problems. The motivation for investigating adaptive techniques arises from the unknown time-varying nature of the tire/road surface interaction that governs vehicle traction. Synchronous application of the engine or brake torques is also proposed for more stable vehicle maneuvers. The lack of controllability during braking (only one net input torque for the two control objectives, i.e., front and rear wheel slips) is partly overcome by applying auxiliary engine torque. Simulations of the two control methods are conducted using a complex nonlinear vehicle model which fully describes the dynamic behavior of the vehicle. Both controllers result in good performance under time-varying operating conditions.**

***Index Terms*—Adaptive fuzzy logic control, adaptive sliding-mode control, intelligent vehicle highway systems (IVHSs), vehicle traction control.**

I. Introduction

THE tire traction force, which controls vehicle longitudinal motion, arises from the tire/road interaction. The tire traction force is proportional to the normal force exerted on the wheel and to the tire/road adhesion coefficient, which depends on the wheel slip (λ), and the road surface condition. Due to the dependency of the longitudinal traction force on λ, traction force control (TFC) can be achieved by controlling λ.

Anti-lock braking systems (ABSs) and traction control, or acceleration slip regulation (ASR), are examples of the state-of-the-art TFCs. However, there are several major difficulties involved in designing a practical TFC algorithm, such as the difficulty of wheel slip estimation and the highly nonlinear and time varying nature of system dynamics. Due to these problems, attempts by several automobile manufacturers to install some versions of ABS or ASR have not met with universal success. These designs were often experimental, rather than analytical, and the tuning and calibration relied essentially on trial and error [1]–[3].

The intelligent vehicle highway system (IVHS) environment provides a reliable and accurate estimate of vehicle speed from magnetic markers equally spaced along the roadway [4]. In turn, this allows for a more accurate estimate of the wheel slip. The IVHS architecture also provides a communication system which allows vehicles on the highway to share driving information, such as the velocity and acceleration of each vehicle, road condition estimates, and obstacle detected by the lead vehicle [5]. These advantages are not available to commercial ABSs, which must operate on limited feedback information. At the same time, the TFC requirement for IVHS applications is much more demanding than that required by commercial ABSs (maximum effort acceleration). For example, TFC must also ensure robust vehicle platooning in this environment (partial effort acceleration).

In this paper, analytical approaches are considered for the design of advanced TFC systems to meet the demands of IVHS operation, primarily from the view point of longitudinal control. Some other point of view in commercial TFC, such as lateral stability under adverse conditions (split-mu or rough road) or human factors are not considered explicitly because these requirements are difficult to meet in analytical study and may be accomplished by experimental tuning. The tire/road surface condition is explicitly considered. Two different approaches are presented. In one case, an approximate tire model is available; and in the other, tire model is not available. For these two cases, ASMC and AFLC are proposed, respectively. These control methods employ different adaptive algorithms to deal with the unknown time-varying tire/road surface condition. In the former case, one parameter (which represents tire/road surface condition in an assumed mathematical tire model) will be estimated; and in the latter, the fuzzy rule base (which includes information of tire/road surface condition) will be adjusted.

For the brakes system, the PATH (Partners for Advanced Transit and Highways) brake control scheme is used [6]. In this scheme, instead of independently controlling the brake pressure applied on each wheel, only the master cylinder is linearly controlled. One limitation of this scheme is the lack of controllability during braking. There are two control objectives (front and rear wheel) even under the bicycle model assumption, while only one control input (the brake torque "or" the engine torque) is available. The application of the engine torque as an auxiliary control during braking is proposed to partly solve this problem.

Simulations are conducted using a complex nonlinear vehicle model for the fastest acceleration/deceleration control and longitudinal platoon control problems. Simulation results show that the TFC with the adaptive algorithms ensures improved stability and robust longitudinal maneuvering.

Manuscript received August 15, 2001; revised February 15, 2002. Abstract published on the Internet November 20, 2002.

H. Lee is with Visteon Corporation, Dearborn, MI 48126 USA (e-mail: hlee11@visteon.com).

M. Tomizuka is with the Department of Mechanical Engineering, University of California, Berkeley, CA 94720 USA.

Digital Object Identifier 10.1109/TIE.2002.807677

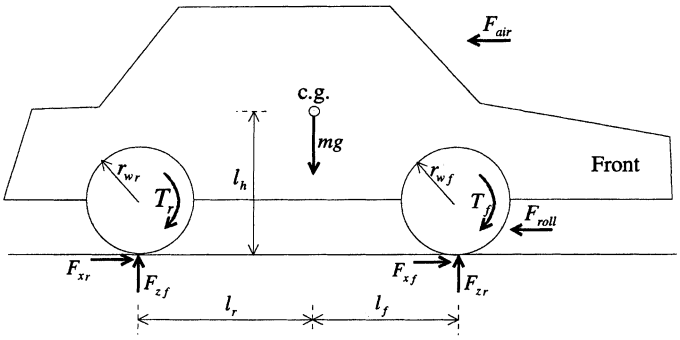

Fig. 1. Schematics of a vehicle model.

II. System Description

A complex vehicle model is utilized to simulate the dynamic behavior of the vehicle as realistically as possible [6]–[8]. This model consists of 12 state variables for six degrees of freedom of the vehicle sprung mass, four wheel states, and two engine states. Additionally, the brake, throttle, and steering actuators are modeled as linear first-order systems. The tire characteristics are obtained from the Bakker–Pacjeka fits of experimental data and the suspension is modeled as four independent spring-damper systems.

From this complex model, we derive the simplified single-track model (Fig. 1) under the following assumptions:

1) neglecting the roll, yaw, lateral, and vertical motion;
2) approximating the normal force as static value;
3) assuming the bicycle model (i.e., the dynamics of the left and right side of the vehicle are identical);
4) discounting the brake, throttle, and steering actuators and manifold dynamics.

Simulations have revealed that the first simplification 1) is valid without any appreciable loss in accuracy under typical to slightly severe environmental conditions. Since the simplified model does not retain suspension dynamics, a static approximation of the normal force 2) at the front and rear wheels is made from the equilibrium of pitch moment around the vehicle center of gravity. If there are no severe steering maneuvers, assumption 3) is also generally valid.

The resulting equations of the simplified vehicle model are

$$m\dot{v}_x = 2\left\lfloor F_{x_f}(\lambda_f) + F_{x_r}(\lambda_r)\right\rfloor - F_{\text{loss}}(v_x) \tag{1}$$

$$J_{wf}\dot{\omega}_{wf} = T_f - r_{wf}F_{x_f}(\lambda_f) \tag{2}$$

$$J_{wr}\dot{\omega}_{wr} = T_r - r_{wr}F_{x_r}(\lambda_r) \tag{3}$$

$$F_{\text{loss}}(v_x) = F_{\text{air}}(v_x) + F_{\text{roll}} = c_x v_x^2 \cdot \text{sgn}(v_x) + f_{\text{roll}}mg \tag{4}$$

$$F_{z_f} = \frac{l_r mg - l_h m\dot{v}_x}{2(l_f + l_r)} = \frac{l_r mg - l_h\left(2\left\lfloor F_{x_f}(\lambda_f) + F_{x_r}(\lambda_r)\right\rfloor - F_{\text{loss}}(v_x)\right)}{2(l_f + l_r)} \tag{5}$$

$$F_{zr} = \frac{l_f mg + l_h m\dot{v}_x}{2(l_f + l_r)} = \frac{l_r mg + l_h\left(2\left\lfloor F_{x_f}(\lambda_f) + F_{x_r}(\lambda_r)\right\rfloor - F_{\text{loss}}(v_x)\right)}{2(l_f + l_r)} \tag{6}$$

where v_x is longitudinal velocity, ω_w is wheel angular velocity, T is input torque on a wheel, F_x is traction force on a wheel, F_z is normal force on a wheel, F_{air} is air drag, and F_{roll} is rolling resistance. The longitudinal wind drag coefficient c_x and rolling resistance coefficient f_{roll} depend on many factors, such as the vehicle shape, the tire temperature, pressure, and material, and the wind gust. Because it is out of the bounds of this paper to investigate the coefficients, some typical numbers are used [16]. Subscripts f and r denote "front tire" and "rear tire," respectively. The vehicle parameters are as follows: m is vehicle mass, c_x is front wind drag coefficient, J_w is the wheel's moment of inertia, r_w is wheel radius, l_f is the distance from the center of gravity (c.g.) to the front axle, l_r is distance from c.g. to the rear axle, and l_h is the vertical distance to c.g. For convenience, subscripts f and r, are not explicitly denoted when both of them are referred to.

Wheel slip, defined by $\lambda \equiv (\omega_w r_w - v_x)/\max(\omega_w r_w, v_x)$, is chosen as the controlled variable for traction control because of its strong influence on the traction. By controlling the wheel slip, the traction force can be indirectly adjusted for the desired output of the system.

By differentiating λ with respect to time, we obtain the wheel slip dynamic equation

$$\dot{\lambda}_f = f_f\left(v_x, \omega_{wf}, \lambda_f, F_{x_f}\right) + h_f(v_x, \omega_{wf}, \lambda_f)T_f \tag{7}$$

$$\dot{\lambda}_r = f_r\left(v_x, \omega_{wr}, \lambda_r, F_{x_r}\right) + h_r(v_x, \omega_{wr}, \lambda_r)T_r \tag{8}$$

where

$$f = -\frac{1}{\omega_w r_w}\left[f_v + \frac{2}{m}\left(F_{x_f} + F_{x_r}\right) + \frac{vr_w}{J_w\omega_w}F_x\right]$$

and

$$h = \frac{vr_w}{J_w(\omega_w r_w)^2}$$

for the acceleration case. f and h are similarly obtained for the deceleration case.

Simulation results depend strongly on the tire model. In this paper, we consider the Bakker–Pacejka fits of experimental data [8]. This tire model can be expressed by the relationship among traction force, tire slip, normal force, and the road condition, i.e.,

$$F_x = f_t(\mu_p, \lambda, F_z) \tag{9}$$

where μ_p is the peak road/tire adhesion coefficient, which indicates the road condition, and takes on values approximately in the interval [0, 1]. Smaller values of μ_p correspond to more slippery road conditions. A simplified tire model will be used for ASMC design

$$F_x = \mu_p \cdot f_t(\lambda, F_z). \tag{10}$$

The shape of the curve have the same form when road surface changes in this simplified model. Fig. 2 shows a typical λ–F_x curve for various road conditions when F_z is fixed.

III. Slip Controller Design

The overall scheme for the proposed control method is shown in Fig. 3.

The control algorithm has to perform two tasks. The first task is to calculate a desired slip ratio λ_{des} based on the aim

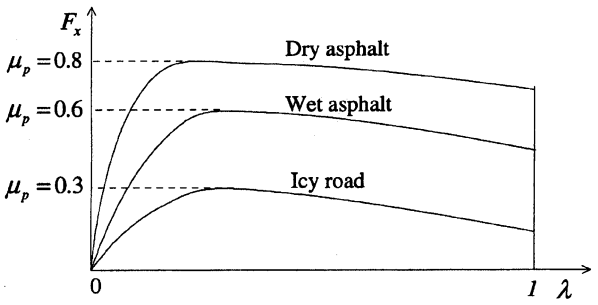

Fig. 2. Typical λ–F_x curve (fixed F_z).

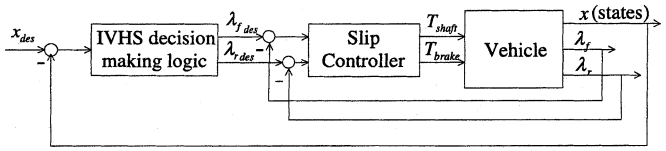

Fig. 3. Block diagram for the proposed control method.

of the TFC and the current states of the vehicle (IVHS decision-making logic). The next task is to actually realize this slip ratio through application of the throttle and brakes (slip controller).

For instance, consider the platooning problem. By the IVHS decision-making logic, a desired traction force is commanded. Since the traction force is a function of λ, the IVHS decision making logic also calculates $\lambda_{\rm des}$ based on the commanded traction force. The slip controller then issues the desired torques at the front and rear wheel, $T_{f_{\rm des}}$ and $T_{r_{\rm des}}$ to drive λ to $\lambda_{\rm des}$. The command inputs to the brake and throttle, $T_{\rm brake_{des}}$ (the *total* available braking torque) and $T_{\rm shaft_{des}}$ (the engine torque exerted on the driving shaft), can be calculated from $T_{f_{\rm des}}$ and $T_{r_{\rm des}}$. These $T_{\rm brake_{des}}$ and $T_{\rm shaft_{des}}$ are achieved by throttle angle control or brake torque control [9].

It should be noted that there are limitations on the possible combinations of T_f and T_r in (2) and (3). In this paper, synchronous application of $T_{\rm brake}$ and $T_{\rm shaft}$ is allowed in order to increase the region of the possible combinations. For example, the engine torque can be an auxiliary control input during deceleration where the brake input alone is not adequate. A particular combination of $T_{\rm brake}$ and $T_{\rm shaft}$ defines an achievable region for $T_{f_{\rm des}}$ and $T_{r_{\rm des}}$. If $T_{f_{\rm des}}$ and $T_{r_{\rm des}}$ violate this possible combination, appropriate optimization depending on each objective is required to correct the combination. Examples of possible combinations of T_f and T_r are shown in Table I for front-wheel-driven (FWD), rear-wheel-driven (RWD), and four-wheel-driven (4WD) vehicles.

The control objective of slip control is to find a control law for the input torque T_f and T_r such that the tracking error $\lambda_{f_e}(t) = \lambda_f(t) - \lambda_{f_{\rm des}}(t)$ and $\lambda_{r_e}(t) = \lambda_r(t) - \lambda_{r_{\rm des}}(t)$, where $\lambda_{f_{\rm des}}$ and $\lambda_{r_{\rm des}}$ are the desired front and rear wheel slip, goes to zero, while all the state variables (v_x, ω_{wf}, ω_{wr}, λ_f, λ_r) remain bounded. Note the following two points related to the system equations.

The system equations are nonlinear and involve uncertainties. Nonlinearities are included from the defining equation of the wheel slip, the tire model, and the functions f_v, fs, and hs.

TABLE I
POSSIBLE COMBINATIONS OF T_f AND T_r

FWD	RWD	4WD
$T_f = 0.5T_{shaft} - 0.3T_{brake}$ $T_r = -0.2T_{brake}$	$T_f = -0.3T_{brake}$ $T_r = 0.5T_{shaft} - 0.2T_{brake}$	$T_f = 4p \sim 6p$ $T_r = 6p \sim 4p$
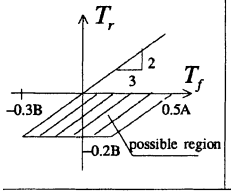	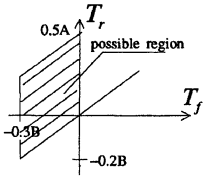	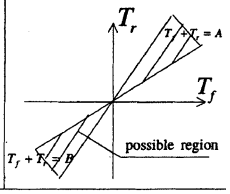

A : $T_{shaft_{\max}}$, B : $T_{brake\max}$

FWD and RWD : Brake torque distribution 60 : 40

4WD : Driving torque distribution ratio 40 : 60 ~ 60 : 40

The traction force, $F_x(\lambda)$, is unknown and time-varying function during driving since it is a function of the road condition (i.e., μ_p) which may be unknown and can be changed during driving.

These properties motivate the use of fuzzy logic control (FLC) as well as sliding-mode control (SMC). Since f is a function of unknown $F_x(\lambda)$, two different cases can be considered for f. In one case, an approximate tire model is available. Therefore, only one parameter μ_p, which represents tire/road surface condition in an assumed mathematical tire model, is unknown. In the other case, the tire model is not available and f is an unknown nonlinear function. For these two cases, adaptive sliding-mode control (ASMC) and adaptive fuzzy logic control (AFLC) are proposed, respectively.

Before deriving the control law for slip control, it is necessary to prove the stability of the internal dynamics.

Lemma: The internal dynamics, (1)–(3), are locally stable in the positive slope region of λ–F_x curve.

Proof: See the Appendix.

A. ASMC

Defining the tracking error vector, $\lambda_e = \lambda - \lambda_{\rm des}$, the slip control problem is to design a control law T which ensures that $\lambda_e \to 0$ as $t \to \infty$.

The sliding surface is defined as

$$s_1 = \lambda_e = 0. \tag{11}$$

In order to obtain the vehicle control, we differentiate this surface and apply the sliding condition

$$\dot{s} = f + hT - \dot{\lambda}_{\rm des} \le -\eta \cdot \mathrm{sgn}(s). \tag{12}$$

The function f (possibly nonlinear or time varying) is not exactly known, but is assumed to be estimated as a function $\hat{f}$. We assume that the estimation error on f is bounded by some known function F:

$$\left|\hat{f} - f\right| \le F. \tag{13}$$

Thus, if we choose input $T_{\rm des}$ as

$$T_{\rm des} = \frac{1}{h}\left[-\hat{f} + \dot{\lambda}_{\rm des} - k \cdot sat\left(\frac{s}{\Phi}\right)\right] \tag{14}$$

where $k = k(\mathbf{x}) = F + \eta$, then the sliding condition may be satisfied. In order to reduce the chattering effect, which results from using the $\mathrm{sgn}(\cdot)$ function in (12), a saturation function is used. In order to estimate f, it is necessary to design an online road condition estimate. Since IVHS decision-making logic frequently produces the desired traction force, $F_{x_{\mathrm{des}}}$, instead of λ_{des}, online road condition estimation is also necessary to calculate λ_{des} from $F_{x_{\mathrm{des}}}$.

Assume that the tire normal forces F_z are known and the aerodynamic drag and the rolling resistance are also well known. Substituting (10) into (1), we have

$$\dot{v}_x = f_v(v_x) + \frac{2}{m}\,\mu_p \cdot \left[f_{t_f}(\lambda_f,\, F_z) + f_{t_r}(\lambda_r,\, F_z)\right]. \quad (15)$$

Defining $y(t)$ as

$$y(t) = \frac{m}{2}\left(\dot{v}_x - f_v(v_x)\right) \quad (16)$$

and assuming that we can measure longitudinal velocity and acceleration $(v_x,\, \dot{v}_x)$, we define $y(t)$ to be the "output signal" of the system. Then, (15) can be expressed in the form

$$y(t) = \mu_p(t) \cdot \phi(t) \quad (17)$$

where $\phi(t) = f_{t_f}(t) + f_{t_r}(t)$.

Note that both $y(t)$ and $\phi(t)$ are assumed to be known from the measurements of the system signals. Thus, the only unknown quantity in (17) is μ_p. Our objective is to determine an adaptation law for the parameter μ_p, which indicates the road condition. Since only one parameter μ_p is required to be adapted, it is not necessary to consider persistent excitation condition unless reference signal $\phi(t)$ is identically zero all the time.

Since the system has the following properties,

- parameter μ_p is a time-varying parameter during driving, because of time-varying road conditions;
- measurements of $y(t)$ and $\phi(t)$ may be contaminated by noise;,

we use a recursive least-squares scheme with a forgetting factor. This method has the capability of estimating time-varying parameters, and it is known to have good robustness with respect to noise and disturbance.

The parameter estimate is generated by minimizing the integral prediction error with the exponential forgetting factor

$$J = \int_0^t \exp\left[-\int_\tau^t \rho(r)\,dr\right] \left\|y(\tau) - \hat{\mu}_p(t)\phi(\tau)\right\|^2 d\tau \quad (18)$$

with respect to $\hat{\mu}_p$, where $\rho(t) \geq 0$ is the time-varying forgetting factor. Note that the exponential term in the integral represents the weighting for the data. It discounts the influence of the past data in the estimation of the current parameter. This property is useful in dealing with a time-varying parameter. The least-squares estimate $\hat{\mu}_p$ satisfies

$$\left[\int_0^t \exp\left[-\int_\tau^t \rho(r)\,dr\right] \phi^2(\tau)\,d\tau\right] \hat{\mu}_p(t) = \int_0^t \exp\left[-\int_\tau^t \rho(r)\,dr\right] \phi(\tau) y(\tau)\,d\tau. \quad (19)$$

Let

$$P(t) = \left[\int_0^t \exp\left[-\int_\tau^t \rho(r)\,dr\right] \phi^2(\tau)\,d\tau\right]^{-1}. \quad (20)$$

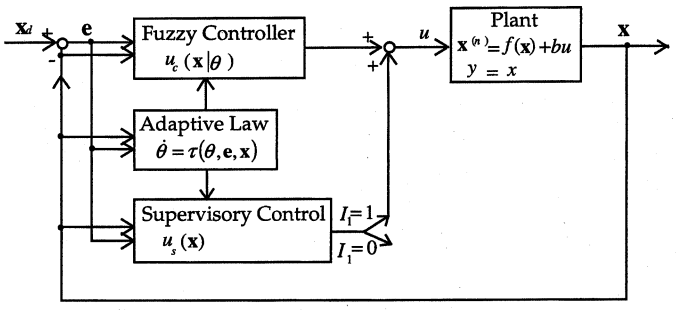

Fig. 4. Overall diagram of direct adaptive fuzzy control.

To achieve computational efficiency, it is desirable to compute $P(t)$ recursively, instead of evaluating the integral at every time instant. This amounts to replacing the above equation by the differential equation

$$\frac{d}{dt}\left[P^{-1}(t)\right] = -\rho(t)P^{-1}(t) + \phi(t)^2. \quad (21)$$

Differentiating (19) and using (20) and (21), the parameter updating and gain updating equations are given by

$$\dot{\hat{\mu}}_p = -P(t)\phi(t)e \quad (22)$$

$$\dot{P}(t) = \rho(t)P(t) - \phi(t)^2 P(t)^2 \quad (23)$$

where $e = \hat{\mu}_p\phi - y$.

B. AFLC

If a tire model is not available, then the f's in (7) and (8) are unknown nonlinear functions. Hence, it is difficult to control slip using a model-based control algorithm. AFLC is proposed in this case.

The overall diagram of the proposed direct adaptive fuzzy controller is shown in Fig. 4.

Consider an nth-order nonlinear system in canonical form

$$x^{(n)} = f\left(x, \dot{x}, \ldots, x^{(n-1)}\right) + h\left(x, \dot{x}, \ldots, x^{(n-1)}\right) u, \qquad y = x \quad (24)$$

where f is an unknown continuous function, and $u \in U$ and $\mathbf{x} \in X$ are the input and states of the system. In our system, x is λ's and u is T_{des}'s.

Assumption: We can determine a function $f^U(\mathbf{x})$ such that $|f(\mathbf{x})| \leq f^U(\mathbf{x})$.

The control u in AFLC is defined as the summation of a fuzzy control $u_c(\mathbf{x}|\Theta)$ and a supervisory control $u_s(\mathbf{x})$

$$u = u_c(\mathbf{x}|\Theta) + u_s(\mathbf{x}) \quad (25)$$

where the supervisory control $u_s(\mathbf{x})$ is introduced in order to guarantee stability of the closed-loop system and to provide fast response [11].

The FLC with *center-average defuzzifier*, *product inference*, and *singleton fuzzifier* [13] is of the following form:

$$u_c(\mathbf{x}|\Theta) = \sum_{l=1}^{M} \overline{u}_c^{\,l}\, \xi^l(\mathbf{x}) = \Theta^T \Xi(\mathbf{x}) \quad (26)$$

where $\Theta = (\overline{u}_c^{\,1}, \ldots, \overline{u}_c^{\,M})^T$ is a parameter vector which is the collection of the points at which the membership functions, $\mu_{H^l}(u_c)$s, achieve their maximum value, M is the number of

rules in the rule base, $\Xi(\mathbf{x}) = (\xi^1(\mathbf{x}), \ldots, \xi^M(\mathbf{x}))^T$, F_i^l and H^l are labels of fuzzy sets in X_i and U, and $\xi^l(\mathbf{x})$'s are the fuzzy basis functions (FBFs, [12]) defined by

$$\xi^l(\mathbf{x}) = \frac{\prod_{i=1}^{n} \mu_{F_i^l}(x_i)}{\sum_{l=1}^{M}\left(\prod_{i=1}^{n} \mu_{F_i^l}(x_i)\right)}. \tag{27}$$

Our purpose is to construct a supervisory control $u_s(\mathbf{x})$ and a fuzzy control $u_c(\mathbf{x}|\Theta)$ by developing an adaptive law for the parameter vector Θ. The following theorem shows the stability of the adaptive fuzzy logic controller [11].

Theorem: Consider the nonlinear plant (24) with control (25), where $u_c(\mathbf{x}|\Theta)$ is given by (26), u_s is given by

$$u_s(\mathbf{x}) = I_1^* \operatorname{sgn}(\mathbf{e}^T\mathbf{p}_n h)\left[|u_c| + \frac{1}{h}\left(f^U + \left|x_d^{(n)}\right| + \left|\mathbf{k}^T\mathbf{e}\right|\right)\right] \tag{28}$$

where $I_1^* = 1$ if $V_e > \overline{V}$, and $I_1^* = 0$ if $V_e \le \overline{V}$ ($\overline{V}$ is a constant specified by the designer), $\mathbf{p}_n$ is the last column of a symmetric positive-definite matrix $\mathbf{P}$, and the parameter vector Θ is adjusted by the adaptive law

$$\dot{\Theta} = \gamma\mathbf{e}^T\mathbf{p}_n\Xi(\mathbf{x}) \quad \text{if } (|\Theta| < M_\theta) \text{ or } (|\Theta| = M_\theta \text{ and } \mathbf{e}^T\mathbf{p}_n\Theta^T\Xi(\mathbf{x}) \le 0) \tag{29}$$

$$\dot{\Theta} = \gamma\mathbf{e}^T\mathbf{p}_n\Xi(\mathbf{x}) - \gamma\mathbf{e}^T\mathbf{p}_n\frac{\Theta\Theta^T\Xi(\mathbf{x})}{|\Theta|^2} \quad \text{if } |\Theta| = M_\theta \text{ and } \mathbf{e}^T\mathbf{p}_n\Theta^T\Xi(\mathbf{x}) > 0 \tag{30}$$

where M_θ is a constant specified by the designer.

Then, there exists a Lyapunov function, $V = (1/2)\mathbf{e}^T\mathbf{P}\mathbf{e} + (b/2\gamma)\Phi^T\Phi$, satisfying

$$\dot{V} \le -\tfrac{1}{2}\,\mathbf{e}^T\mathbf{Q}\mathbf{e} - \mathbf{e}^T\mathbf{P}\mathbf{b}_c w \tag{31}$$

where

$$w \equiv u_c(\mathbf{x}|\Theta^*) - u^*, \quad \Theta^* \equiv \underset{|\Theta|\le M_\theta}{\operatorname{argmin}}\left[\sup_{|\mathbf{x}|\le M_x} |u_c(\mathbf{x}|\Theta) - u^*|\right]$$

and $\Phi \equiv \Theta^* - \Theta$.

Proof: Given in [11].

From the Universal Approximation Theorem [12], we can expect that the w should be small enough to get $\dot{V} \le 0$, provided that we use sufficiently complex $u_c(\mathbf{x}|\Theta^*)$ (in terms of number of adjustable parameters). In order to guarantee $|\Theta| \le M_\theta$, we use a projection algorithm as given (29) and (30).

$\lambda_e = \lambda - \lambda_{\text{des}}$ is chosen as the input fuzzy variable for the fuzzy logic wheel slip control. Five fuzzy control rules $(M = 5)$ are derived by engineering judgment.

Rule 1) IF λ_e is NB, THEN T_{des} is PB.
Rule 2) IF λ_e is NS, THEN T_{des} is PS.
Rule 3) IF λ_e is ZO, THEN T_{des} is ZO.
Rule 4) IF λ_e is PS, THEN T_{des} is NS.
Rule 5) IF λ_e is PB, THEN T_{des} is NB.

For example, if λ_e is positive big (PB), then the input torque should be decreased (T_{des} = NB) since decreasing input torque makes the slip decrease. We define five fuzzy sets over interval $[-2, 2]$, with labels NB (negative big), NS (negative small), ZO (zero), PS (positive small), PB (positive big). Fuzzy membership functions for these labels are

$$\mu_{NB} = \frac{1}{1+e^{5(x+1)}}$$
$$NS = e^{-(x+1)^2}$$
$$\mu_{ZO} = e^{-(x+0)^2}$$
$$\mu_{PS} = e^{-(x-1)^2}$$
$$\mu_{PB} = \frac{1}{1+e^{-5(x-1)}}.$$

IV. Applications and Simulations

Vehicle velocity (v_x) and wheel angular velocity (w_w) are assumed to be estimated exactly in IVHS [4]. The tire model obtained in (9) is assumed to be the real tire model. Analytical approximations of the real road conditions can be denoted as

$$dry\ asphalt: \quad \mu_p = 0.8;$$
$$wet\ asphalt: \quad \mu_p = 0.5;$$
$$icy\ road: \quad \mu_p = 0.3.$$

A. Fastest Acceleration/Deceleration Control

The objective of fastest acceleration/deceleration control is to maximize the magnitude of the traction force. These maximum traction forces are achieved at the negative or positive peak point of the λ–F_x curve. Therefore, to produce the fastest acceleration, the wheel slip should be regulated where the traction force attains the peak value. Since the peak value of λ varies depending on the tire characteristics, the road condition, and the normal force exerted at the tire, it is generally unknown during driving. Therefore, fastest acceleration/deceleration control includes searching for and maintaining the peak slip.

The peak seeking and maintaining strategy includes the following three steps.

1) Estimate the local slope in the λ—F_x curve.
2) Move the target slip in the estimated direction toward the peak slip.
3) Steer the wheel slip toward the new target slip via sliding mode or fuzzy logic slip control and then return to 1).

The remaining task is to calculate $T_{\text{shaft}_{\text{des}}}$ and $T_{\text{brake}_{\text{des}}}$ from $T_{f_{\text{des}}}$ and $T_{r_{\text{des}}}$. Generally, under the 60/40 braking torque distribution, the rear wheel slip ratio may be saturated (skidding) during braking before front wheel slip ratio reaches its peak value. Therefore, for RWD or 4WD vehicle, rear wheel slip saturation can be eliminated and both (front and rear) wheel slip ratios can be maintained at their peak values by applying synchronous engine torque to the rear wheel (RWD), or by changing braking torque distribution (4WD). However, for the FWD vehicle, it is necessary to optimize the distribution of $T_{f_{\text{des}}}$ and $T_{r_{\text{des}}}$ so that the combination of $T_{f_{\text{des}}}$ and $T_{r_{\text{des}}}$ is located in the possible region in Table I.

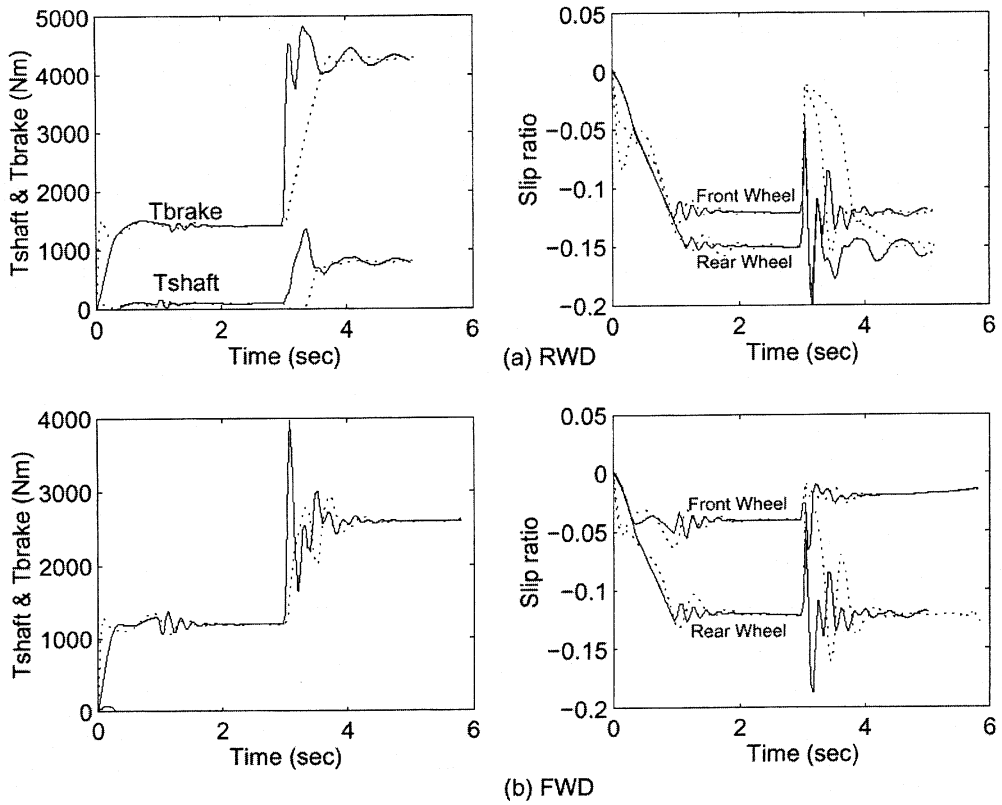

Fig. 5. Fastest deceleration control (solid line: ASMC; dotted line: AFLC) (peak slip: front = −0.15; rear = −0.12).

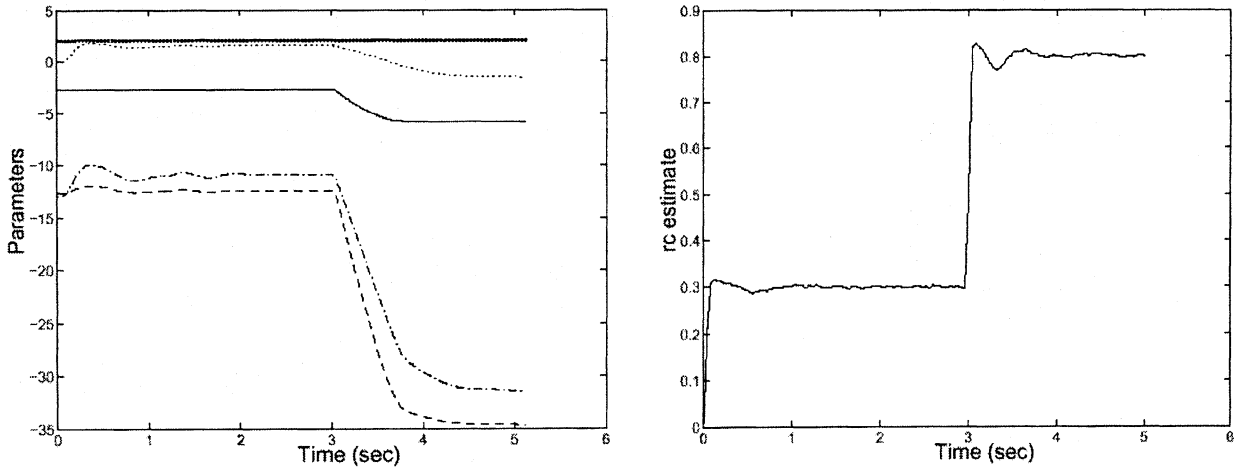

Fig. 6. Parameter adaptation. (a) Adaptation parameter of AFLC. (b) μ_p estimate of ASMC.

The simulation results using ASMC and AFLC are shown in Fig. 5. The road condition is assumed to be changed at 3 s from icy road to dry asphalt. The simulations were conducted until vehicle velocity reached 5 m/s from 30 m/s. Each control results in good performance in searching for and maintaining the peak slip value. When road conditions are changed, each controller keeps the peak slip again after a short transient state. As mentioned before, synchronous engine torque is applied to the RWD vehicle in order to prevent the rear wheels from skidding. The control criterion for the FWD vehicle is not fastest deceleration but vehicle stability, which means prohibiting rear wheels from skidding. The updating process of the five parameters ($\overline{u}_c^l$s) of AFLC and road condition estimate ($\hat{\mu}_p$) of ASMC is presented in Fig. 6. $\hat{\mu}_p$ converges to its first real value (0.3) and quickly adapts to its final value. $\overline{u}_c^l$'s are also updated after road condition change.

The simulation results of standard (i.e., without adaptive algorithm) FLC and SMC are shown in Fig. 7 for the RWD vehicle. The nominal road condition for SMC design was assumed to be wet asphalt ($\mu_p = 0.6$). Initial fuzzy rules for FLC were tuned to icy road conditions. These standard controllers result in input torque chattering and cannot be adapted to a new con-

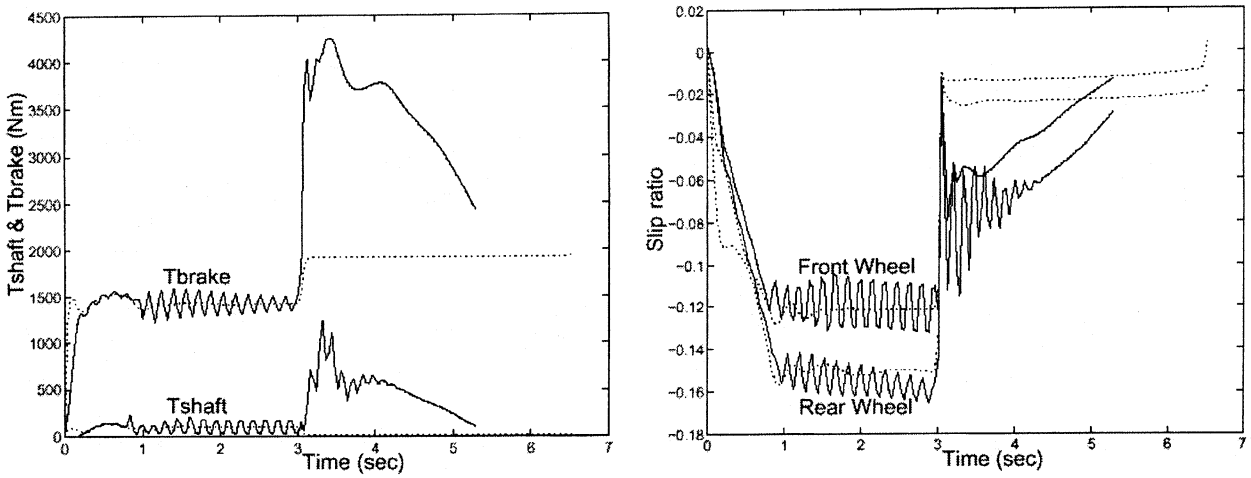

Fig. 7. Fastest deceleration control (solid line: SMC; dotted line: FLC) (peak slip: front = −0.15; rear = −0.12).

dition. Furthermore, the required time of standard controllers to decelerate the vehicle from $v = 30$ m/s to $v = 5$ m/s, is longer than that for adaptive controllers (SMC: 5.32 s; FLC: 6.53 s; ASMC: 5.03 s; AFLC: 5.15 s).

B. Longitudinal Platoon Control

Longitudinal control strategies are necessary in order to regulate the spacing and velocity of vehicles in a platoon in an automated highway system [14]. The controller must also ensure good performance over a variety of operating points and external conditions without sacrificing safety or reliability.

Some research has been performed on this topic via simulations and experiments [5], [15]. However, previous work did not emphasize adverse road conditions or road condition changes. The objective of this section is to show the possibility of using adaptive control algorithms to deal with the unknown time-varying road condition in the longitudinal platoon control. The two-car platoon will be considered in what follows.

The spacing error is defined as

$$\varepsilon(t) = x(t) - (x_{\text{lead}}(t) - x_{\text{spacing}}) \tag{32}$$

where x_{space} is a constant desired spacing between two vehicles, $x(t)$ is the following controlled vehicle location, and $x_{\text{lead}}(t)$ is the lead vehicle location. Since the control task of the platoon control is to track the velocity of the leading vehicle while maintaining a constant separation, an obvious choice for a sliding surface is one which incorporates the corresponding errors. Let the sliding surface be defined as

$$s_1 = \dot{\varepsilon} + 2c_1\varepsilon + c_1^2 \int_0^t \varepsilon\, dt = 0 \tag{33}$$

where $\dot{\varepsilon} = \dot{x} - \dot{x}_{\text{lead}} = v_x - v_{x_{\text{lead}}}$.

Differentiating (33) and considering the sliding condition yields

$$\dot{s}_1 = \frac{2}{m}\left[F_{x_f}(\lambda_f) + F_{x_r}(\lambda_r)\right] - \frac{1}{m}F_{\text{loss}} - a_{\text{lead}} + 2c_1\dot{\varepsilon} + c_1^2\varepsilon \leq -\eta_1 sat\left(\frac{s_1}{\Phi}\right). \tag{34}$$

Then, the desired traction force is

$$\left(F_{x_f} + F_{x_r}\right)_{\text{des}} = -\frac{m}{2}\left[-\frac{1}{m}F_{\text{loss}} - a_{\text{lead}} + 2c_1\dot{\varepsilon} + c_1^2\varepsilon + \eta_1 sat\left(\frac{s_1}{\Phi}\right)\right]. \tag{35}$$

The next step is calculation of $\lambda_{f_{\text{des}}}$ and $\lambda_{r_{\text{des}}}$ from $(F_{x_f} + F_{x_r})_{\text{des}}$. From (10) and Fig. 2, the following relationship should be maintained during deceleration (note $F_{x_f} \leq 0$ and $F_{x_r} \leq 0$):

$$F_{x_f} \geq -\mu_p f_{t_f}(F_{z_f}, \lambda_{pf}) \approx -\mu_p F_{zf} \tag{36}$$

$$F_{x_r} \geq -\mu_p f_{t_r}(F_{z_r}, \lambda_{pr}) \approx -\mu_p F_{z_r}. \tag{37}$$

Then, from (5) and (6),

$$F_{x_f} \geq -\mu_p \frac{l_r mg - 2l_h F_{x_r} + l_h F_{\text{loss}}}{2(l_f + l_r - \mu_p l_h)} \tag{38}$$

$$F_{x_r} \geq -\mu_p \frac{l_f mg + 2l_h F_{x_f} - l_h F_{\text{loss}}}{2(l_f + l_r + \mu_p l_h)}. \tag{39}$$

The optimal tire force distribution to achieve the best deceleration response can be obtained from the intersection point of the two boundary lines of (38) and (39)

$$\frac{F_{x_f}}{F_{x_r}} = \frac{l_r + l_h f_{\text{loss}} + \mu_p l_h}{l_f - l_h f_{\text{loss}} - \mu_p l_h} \tag{40}$$

where $f_{\text{loss}} = F_{\text{loss}}/mg$. $\lambda_{f_{\text{des}}}$ and $\lambda_{r_{\text{des}}}$ can be obtained from (35), (36), (22), and (10). A similar equation such as (40) can be obtained for the acceleration case.

Simulations were conducted to show the effect of traction control on longitudinal platoon control. Fig. 8 shows the results of platoon control for the icy road and a mild decelerating maneuver. ASMC and AFLC result in similar performance when the assumed tire model in ASMC is exactly same as the real model. The updating process of the five parameters ($\overline{u}_c^l$s) of AFLC and road condition estimate ($\hat{\mu}_p$) of ASMC is presented

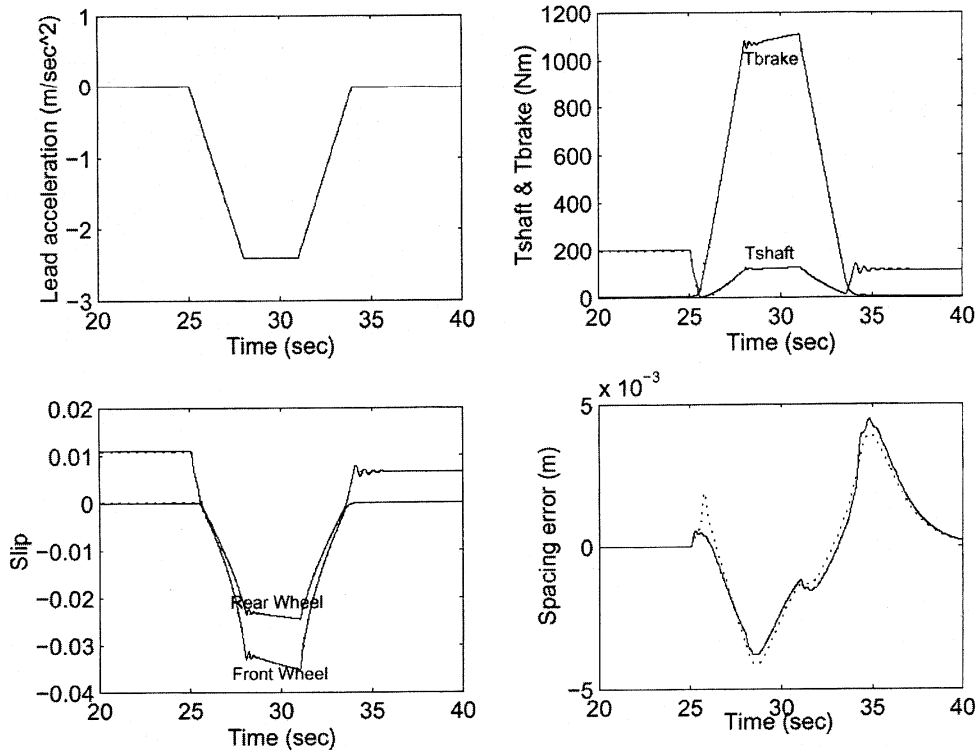

Fig. 8. Longitudinal platoon control (assumed tire = real tire) (solid line: ASMC; dotted line: AFLC).

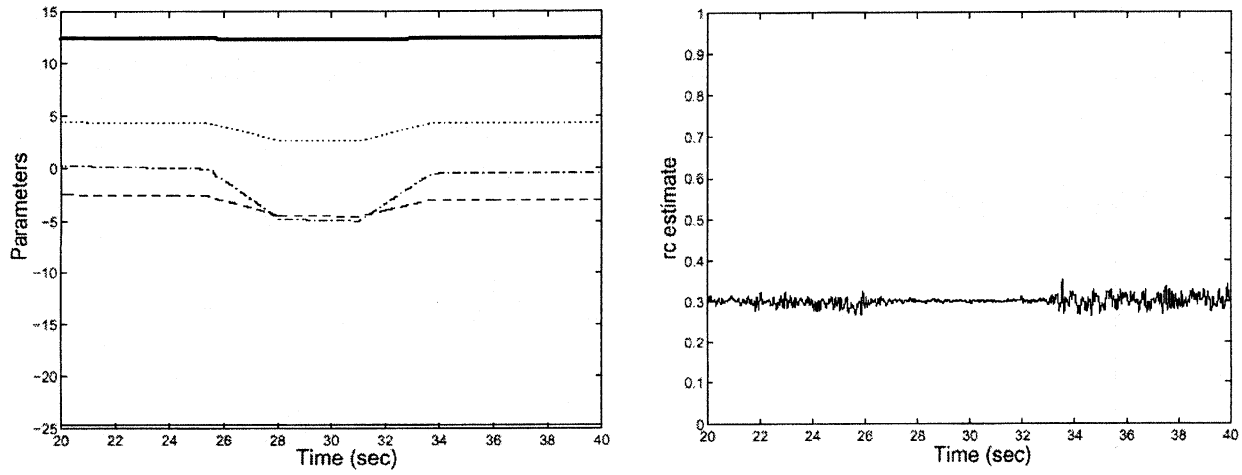

(a) (b)

Fig. 9. Parameter adaptation. (a) Parameter adaptation parameter of AFLC. (b) μ_p estimate of ASMC.

in Fig. 9. $\hat{\mu}_p$ converges to its correct value (0.3) even under measurement noise. However, if the assumed tire model is different from the real model, such as in the first figure in Fig. 10, $\hat{\mu}_p$ does not converge to the correct value. This incorrectly estimated $\hat{\mu}_p$ results in bad performance, i.e., input torque chatter and increased spacing error, while AFLC maintains its performance.

A comparison of the results between TFC and Non-TFC is shown in Fig. 11 under adverse driving conditions (icy road and severe braking). TFC reduces the spacing error. At the same time, it prevents tires from skidding or locking while Non-TFC results in severe rear wheel skidding. Therefore, application of TFC to longitudinal platoon control is an important design consideration in enhancing the vehicle stability.

V. Conclusion

Traction force controller design for longitudinal control of vehicles in automated highway systems was presented. Two control strategies, AFLC and ASMC, were studied for slip control, which in turn controls the traction force. Adaptive algorithms were introduced to each of the control methods to deal with the unknown interaction between the tires and the road surface.

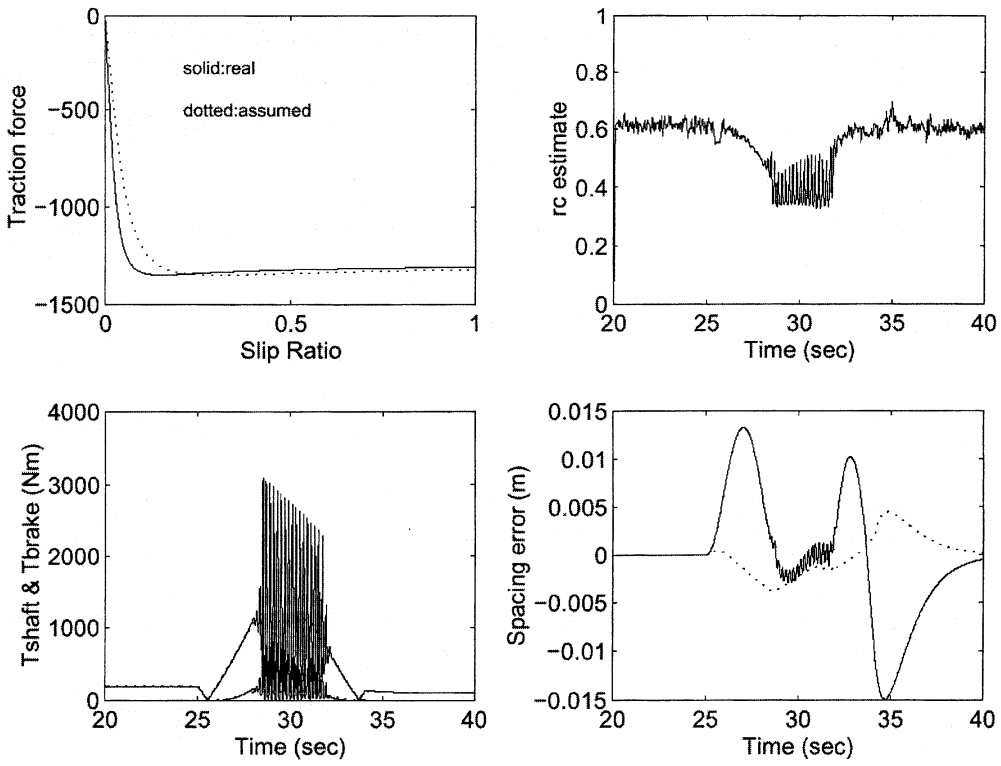

Fig. 10. Longitudinal platoon control (assumed tire $\neq$ real tire) (solid line: ASMC; dotted line: AFLC).

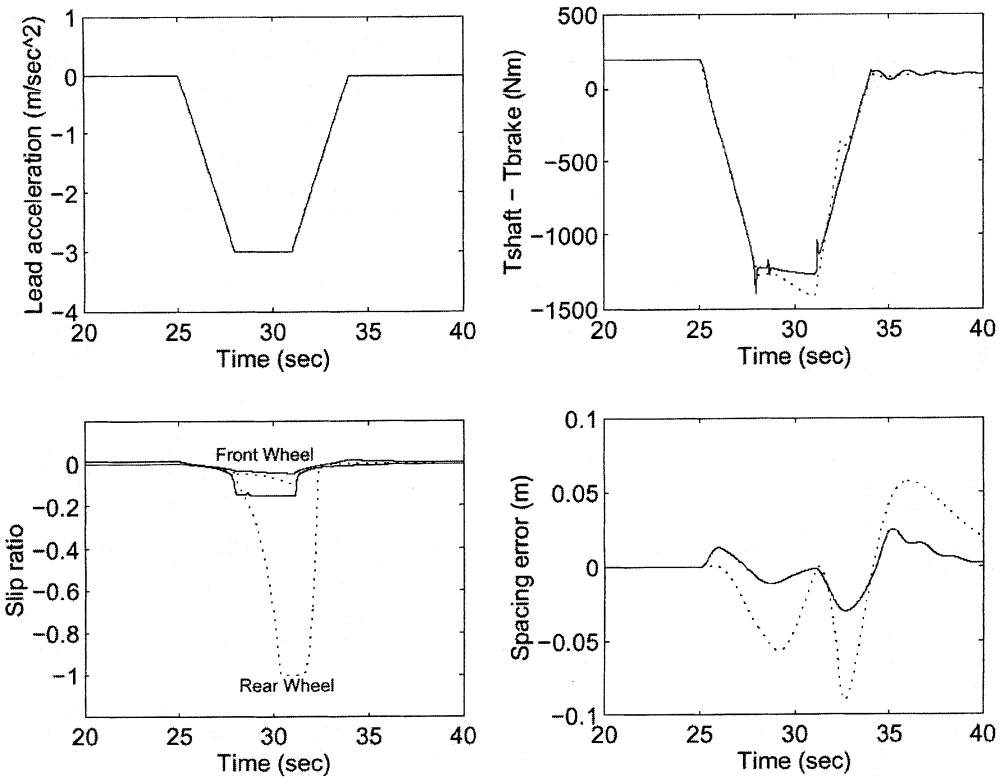

Fig. 11. Longitudinal platoon control (solid line: TFC; dotted line: non-TFC).

These controllers were designed from a simplified vehicle model and applied for simulations to the complex vehicle model to show how these traction control algorithms can be used to satisfy different objectives of vehicle longitudinal control. Simulation results show that the ATFC, including adaptive algorithms, gives more stable and robust longitu-

dinal maneuvering than nonadaptive TFC or non-TFC. ATFC searches for and maintains the peak slip value which gives the maximum tire traction force for the fastest deceleration even under changing road condition. ATFC also prevents skidding and reduces the spacing error of vehicle platooning while Non-TFC causes severe tire skid or unacceptable spacing error under adverse driving conditions. TFC can also quickly adapt to new conditions when tire/road conditions are changing.

The comparative study between ASMC and AFLC shows that each control method has its own advantages and disadvantages, depending on the objectives considered. If a reliable tire model is available, model-based control such as ASMC results in better performance, with respect to faster parameter adaptation or relaxing the persistent excitation condition. But, if a tire model is not available, the only choice is to use high gain control or knowledge-based control, such as AFLC.

APPENDIX

PROOF OF LEMMA

Let $\mathbf{x} = (x_1 \;\; x_2 \;\; x_3)^T = (mv_x \;\; J_{wf}\omega_{wf} \;\; J_{wr}\omega_{wr})^T$. The system dynamics can be written as

$$\dot{\mathbf{x}} = \mathbf{f}(\mathbf{x}) + \mathbf{h}\mathbf{T} \tag{a1}$$

where

$$\mathbf{f}(\mathbf{x}) = \left(f_v(v_x) + \frac{2}{m}\left[F_{x_f}(\lambda_f) + F_{x_r}(\lambda_r)\right] \right.$$
$$\left. -r_{wf}\, F_{x_f}(\lambda_f) \; r_{wr} F_{x_r}(\lambda_r) \right)^T$$

$$\mathbf{h} = \begin{pmatrix} 0 & 0 \\ 1 & 0 \\ 0 & 1 \end{pmatrix}$$

and $\mathbf{T} = (T_f \;\; T_r)^T$. The equilibrium point $\mathbf{x}_o$ for nominal inputs, $\mathbf{T}_0$, is obtained by equating the right-hand sides of (1)–(3) to zero. Therefore,

$$(T_f + T_r)_0 = \frac{r_w}{2} F_{\text{loss}}. \tag{a2}$$

Then, (a1) can be linearized at the equilibrium point as

$$\dot{\mathbf{x}} = \mathbf{A} + \mathbf{g}\mathbf{T} \tag{a3}$$

where the Jacobian matrix

$$\mathbf{A} = \left(\frac{\partial \mathbf{f}(\mathbf{x})}{\partial \mathbf{x}} \right)_{\mathbf{x}_0, \mathbf{T}_0}.$$

From Lyapunov's linearization method, the equilibrium point is locally asymptotically stable for the actual nonlinear system (a1) if the linearized system (a3) is asymptotically stable [10]. For the acceleration case, the Jacobian matrix at $\mathbf{x}_o$ is

$$\mathbf{A} = \begin{pmatrix} a & b & c \\ d & e & 0 \\ f & 0 & g \end{pmatrix}_{\mathbf{x}_0, \mathbf{T}_0} \tag{a4}$$

where

$$a = \frac{\partial f_v}{\partial x_1} + \frac{2}{m}\left[\frac{\partial F_{x_f}}{\partial \lambda_f}\frac{\partial \lambda_f}{\partial x_1} + \frac{\partial F_{x_r}}{\partial \lambda_r}\frac{\partial \lambda_r}{\partial x_1}\right]$$
$$b = \frac{2}{m}\left(\frac{\partial F_{x_f}}{\partial \lambda_f}\frac{\partial \lambda_f}{\partial x_2}\right)$$
$$c = \frac{2}{m}\left(\frac{\partial F_{x_r}}{\partial \lambda_r}\frac{\partial \lambda_r}{\partial x_3}\right)$$
$$d = -r_f \frac{\partial F_{x_f}}{\partial \lambda_f}\frac{\partial \lambda_f}{\partial x_1}$$
$$e = -r_f \frac{\partial F_{x_f}}{\partial \lambda_f}\frac{\partial \lambda_f}{\partial x_2}$$
$$f = -r_r \frac{\partial F_{x_r}}{\partial \lambda_r}\frac{\partial \lambda_r}{\partial x_1}$$

and

$$g = -r_r \frac{\partial F_{x_r}}{\partial \lambda_r}\frac{\partial \lambda_r}{\partial x_3}.$$

The characteristic equation $\det(s\mathbf{I} - \mathbf{A}) = 0$ is

$$s^3 - (a+e+g)s^2 + (ae+ag+eg-bd-cf)s + (-ceg+bdg+cef) = 0. \tag{a5}$$

From Routh–Hurwitz criterion, (a3) is asymptotically stable if and only if

$$-(a+e+g) > 0 \tag{a6}$$
$$(ae+ag+eg-bd-cf) > 0 \tag{a7}$$
$$(-ceg+bdg+cef) > 0 \tag{a8}$$
$$-(a+e+g)(ae+ag+eg-bd-cf) - (-ceg+bdg+cef) > 0. \tag{a9}$$

It can be easily proved that above conditions, (a6)∼(a9), are satisfied if $\partial F_{x_f}/\partial \lambda_f > 0$ and $\partial F_{x_r}/\partial \lambda_r > 0$. Similar result can be obtained for the deceleration case.

REFERENCES

[1] H. Leiber and A. Czinczel, "Four years of experience with 4-wheel anti-skid brake (ABS)," Soc. Automotive Eng., SAE Paper 830481, 1983.

[2] S. Yoneda, Y. Naitoh, and H. Kigoshi, "Rear brake lock-up control system of Mitsubishi Starion," Soc. Automotive Eng., SAE Paper 830482, 1983.

[3] D. R. McLellan *et al.*, "Increasing the safe driving envelope—ABS, traction control and beyond," in *Proc. 1992 Int. Congr. Transportation Electronics*, Dearborn, MI, Oct. 1992, pp. 103–124.

[4] H. Lee, D. Love, and M. Tomizuka, "Longitudinal maneuvering control for automated highway systems based on a magnetic reference/sensing system," in *Proc. 1995 American Control Conf.*, Seattle, WA, 1995, pp. 150–154.

[5] K. S. Chang *et al.*, "Experimentation with a vehicle platoon control system," in *Proc. 1991 Vehicle Navigation and Information System Conf.*, Dearborn, MI, 1991, pp. 1117–1124.

[6] S. B. Choi and P. Devlin, "Throttle and brake combined control for intelligent vehicle highway systems," Soc. Automotive Eng., SAE Paper 951897, 1995.

[7] M. Tomizuka, J. K. Hedrick, and H. Pham, "Integrated maneuvering control for automated highway systems based on a magnetic reference/sensing system," Univ. California, Berkeley, CA, PATH Rep. UCB-ITS-PRR-95-12, 1995.

[8] H. Peng and M. Tomizuka, "Lateral control of front-wheel-steering rubber-tire vehicles," Univ. California, Berkeley, CA, PATH Rep. UCB-ITS-PRR-90-5, 1990.
[9] H. Lee and M. Tomizuka, "Adaptive traction control," Univ. California, Berkeley, CA, PATH Rep. UCB-ITS-PRR-95-32, 1995.
[10] J.-J. E. Slotine and W. Li, *Applied Nonlinear Control*. Englewood Cliffs, NJ: Prentice-Hall, 1991.
[11] L.-X. Wang, "Stable adaptive fuzzy control of nonlinear systems," *IEEE Trans. Fuzzy Syst.*, vol. 1, pp. 146–155, May 1993.
[12] L.-X. Wang and J. M. Mendel, "Fuzzy basis functions, universal approximation, and orthogonal least squares learning," *IEEE Trans. Neural Networks*, vol. 3, pp. 807–814, Sept. 1992.
[13] C. Lee, "Fuzzy logic in control systems: Fuzzy logic controller—Part I," *IEEE Trans. Syst., Man, Cybern.*, vol. 20, pp. 404–418, Mar. 1990.
[14] S. Sladover *et al.*, "Automatic vehicle control developments in the PATH program," *IEEE Trans. Veh. Technol.*, vol. 40, pp. 114–130, Feb. 1991.
[15] D. Swaroop and J. K. Hedrick, "Direct adaptive longitudinal control for vehicle platoons," in *Proc. IEEE Conf. Decision and Control*, Dec. 1994, pp. 684–689.
[16] T. D. Gillespie, *Fundamentals of Vehicle Dynamics*. Warrendale, PA: SAE, 1992.

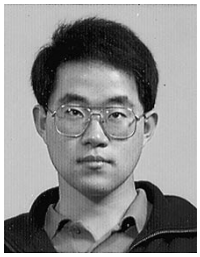

Hyeongcheol Lee was born in Seoul, Korea, in 1965. He received the B.S. and M.S. degrees from Seoul National University, Seoul, Korea, in 1988 and 1990, respectively, and the Ph.D. degree from the University of California, Berkeley, in 1997.

He is currently a Technical Fellow with Visteon Corporation, Dearborn, MI. His research interests include adaptive and nonlinear control, applications to automotive vehicle controls, and vehicle dynamics.

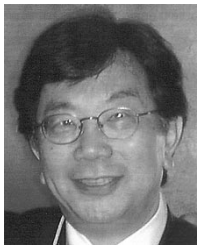

Masayoshi Tomizuka (M'86–SM'95–F'97) was born in Tokyo, Japan, in 1946. He received the B.S. and M.S. degrees from Keio University, Tokyo, Japan, and the Ph.D. degree in 1974 from Massachusetts Institute of Technology, Cambridge, all in mechanical engineering.

In 1974, he joined the faculty of the Department of Mechanical Engineering, University of California, Berkeley, where he currently holds the Cheryl and John Neerhout, Jr., Distinguished Professorship Chair. At the University of California, he teaches courses in dynamic systems and controls. His current research interests are optimal and adaptive control, digital control, signal processing, motion control, and control problems related to robotics, machining, manufacturing, information storage devices and vehicles. He has served as a Consultant to various organizations, including the Lawrence Berkeley Laboratory, General Electric, General Motors, and United Technologies.

Prof. Tomizuka served as Technical Editor of the *ASME Journal of Dynamic Systems, Measurement and Control*, (J-DSMC) (1988–1993), Editor-in-Chief of the IEEE/ASME TRANSACTIONS ON MECHATRONICS (1997–1999), and an Associate Editor of the *Journal of the International Federation of Automatic Control*, *Automatica*, and the *European Journal of Control*. He was General Chairman of the 1995 American Control Conference, and served as President of the American Automatic Control Council (1998–1999). He is a Fellow of the American Society of Mechanical Engineers (ASME) and the Society of Manufacturing Engineers. He is the recipient of the J-DSMC Best Paper Award (1995), the Dynamic Systems and Control Division (DSCD) Outstanding Investigator Award (ASME, 1996), the Charles Russ Richards Memorial Award (ASME, 1997) and the Rufus Oldenburger Medal (ASME, 2002).